Achieving Large Uniform Tensile Ductility in Nanocrystalline Metals

Y. M. Wang,[1,*] R. T. Ott,[2,†] A. V. Hamza,[1] M. F. Besser,[2] J. Almer,[3] and M. J. Kramer[2]

[1]*Physical and Life Sciences Directorate, Lawrence Livermore National Laboratory, Livermore, California 94550, USA*
[2]*Division of Materials Science and Engineering, Ames Laboratory (USDOE), Ames, Iowa 50011, USA*
[3]*Advanced Photon Source, Argonne National Laboratory, Argonne, Illinois 60439, USA*

(Received 20 January 2010; published 17 November 2010)

Synchrotron x-ray diffraction and high-resolution electron microscopy revealed the origin of different strain hardening behaviors (and dissimilar tensile ductility) in nanocrystalline Ni and nanocrystalline Co. Planar defect accumulations and texture evolution were observed in Co but not in Ni, suggesting that interfacial defects are an effective passage to promote strain hardening in truly nanograins. Twinning becomes less significant in Co when grain sizes reduce to below ~15 nm. This study offers insights into achieving excellent mechanical properties in nanocrystalline materials.

DOI: 10.1103/PhysRevLett.105.215502 PACS numbers: 62.20.F−, 61.46.Hk

Although inspiring progress has been made in achieving extraordinary mechanical properties in nanocrystalline (NC) solids (grain sizes $D < 100$ nm), the lack of tensile ductility in NC metals remains a long-standing problem [1]. This obvious shortcoming is widely attributed to their lack of strain hardening; i.e., a large amount of dislocation storage has not been realistic in most NC metals. This is especially true when D decreases below ~30 nm—a regime where the grain boundaries (GBs) become dominant sources or sinks for dislocations. In some other cases, however, large strain hardening and uniform tensile elongation ($\varepsilon_{\text{unif}}$) have been observed in NC metals [2–4]. The physical origin of these experimental observations unfortunately remains speculative. Recently, strain hardening and dislocation accumulations through a Lomer-Cottrell lock mechanism were reported in cryogenic-rolled NC-Ni ($D \sim 20$ nm) [5]. The general implications of these results in enhancing the $\varepsilon_{\text{unif}}$ of NC metals remain uncertain however, as NC-Ni exhibits a persistently low $\varepsilon_{\text{unif}}(<2\%)$ even at cryogenic temperatures [6]. Collectively, these ongoing investigations suggest that various deformation mechanisms (DMs) reported so far under nontensile conditions may bear less implication to tensile plasticity due to clearly different achievable strain levels and possible tension-compression asymmetry. The loading mode becomes more problematic in hexagonal close-packed (hcp) metals, where different slip/twinning systems are operative under tension or compression. These load-dependent DMs in NC metals underscore the importance of using *in situ* tensile experiments to investigate the relevant DMs.

Here we study the DMs of NC-Ni and NC-Co through synchrotron x-ray diffraction (SXRD) experiments with the key aim to uncover the physical origin of their intrinsic differences in strain hardening and resultant tensile plasticity. Both metals are electrodeposited with clean grain interiors. The face-centered cubic (fcc) NC-Ni is from the same batch as reported in Ref. [6]. Transmission electron microscopy (TEM) examinations indicate that it has a D distribution (29 ± 11 nm; ~25 nm from SXRD data). The as-synthesized hcp NC-Co has an average D of 20 ± 9 nm, and contains a negligible amount (< 0.5%) of fcc phase evidenced by the small $(200)_{\text{fcc}}$ peak in the SXRD data shown in Fig. 1(a). This low-intensity peak was not revealed previously by conventional Cu K_α XRD [3], but is consistent with a few growth twins observable in TEM images. The NC-Ni has a weak (111) in-plane peak based on the (111) intensity ratio relative to other peaks. Room-temperature quasistatic tensile tests at a strain rate of 1.1×10^{-4} s^{-1} displayed in Fig. 1(b) indicate that both NC metals exhibit appreciable strain hardening immediately following macroscopic yielding, but head off to clearly different trends as the plastic strain progresses, leading to an eminent disparity in tensile ductility; i.e., the achievable $\varepsilon_{\text{unif}}$ of NC-Co (~ 8.4%) is about 3 times larger than that of NC-Ni (~ 2.7%). The inset of Fig. 1(b) summarizes the yield strength (σ_y) vs $\varepsilon_{\text{unif}}$ for various NC metals with an average $D < 30$ nm, showing a few examples of large-$\varepsilon_{\text{unif}}$ (> 5%) metals, including NC-Cu [2], NC-Co [3], and NC-Ni-Fe [4]. Earlier work attributes this intriguing large $\varepsilon_{\text{unif}}$ to various reasons such as dislocation-trapping [2], twinning [3], and/or sample quality [4], but no direct evidence was obtained. The high-energy ($E = 80.715$ keV, 0.153 589 Å wavelength) x-rays at sector 1 of the Advanced Photon Source enables real-time tracking of the lattice strain and peak intensity in NC metals during tensile loading (the sample gauge section is ~4.5 mm long × 2.2 mm wide × 0.13 mm thick). The samples were loaded in a MTS 858 frame, while the diffracted intensity from the samples was collected on an amorphous Si detector (41 × 41 cm^2 in area) positioned 1103 mm from the NC-Ni and 970 mm from the NC-Co. The pixel size of the camera is 200×200 μm^2. The Q-space resolution for both camera lengths is better than ~0.01 Å^{-1}.

For SXRD studies, a useful parameter for understanding DMs is the in-plane lattice strain, which is defined as $\varepsilon^{hkl} = (d^{hkl} - d_0^{hkl})/d_0^{hkl}$, where hkl denotes grains with

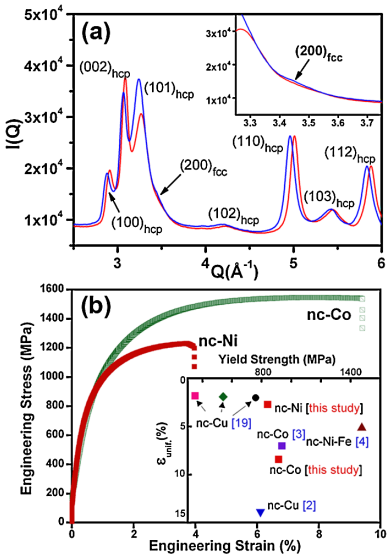

FIG. 1 (color online). (a) SXRD spectra for NC-Co at 0% (red line) and 2.5% (blue line) strains (corresponding stress levels of 0 and 1365 MPa, respectively). The inset is a zoomed-in region of the $(200)_{\mathrm{fcc}}$ peak, showing a slight change of the peak intensity during straining. (b) Engineering stress-strain plots of NC-Ni and NC-Co, respectively. The inset is a summary of $\sigma_{0.2\%}$ vs $\varepsilon_{\mathrm{unif}}$ for various NC metals with an average $D < 30$ nm.

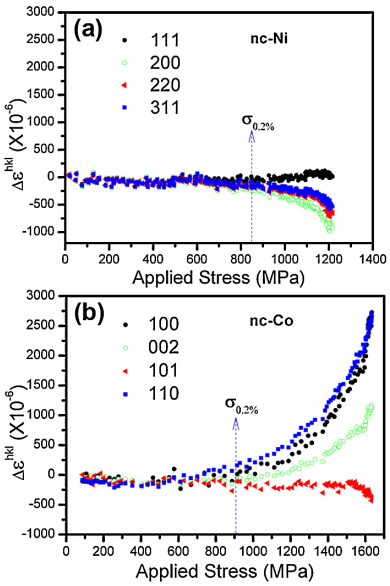

FIG. 2 (color online). The $\Delta\varepsilon^{hkl}$ (shown in the same scale range) as a function of the applied stress for (a) NC-Ni and (b) NC-Co.

(hkl) planes normal to the direction of the x-ray scattering vector (Q^{hkl}), and d_0^{hkl} and d^{hkl} are the interplanar spacing before and during loading, respectively [4,7,8]. The deviation of ε^{hkl} from linear elasticity (i.e., $\Delta\varepsilon^{hkl} = \varepsilon^{hkl} - \sigma_A/E^{hkl}$, where σ_A is the applied stress and E^{hkl} the calculated elastic response for a specific hkl) reflects the yielding and is caused by the elastic and plastic anisotropy developed inside various grain families. Figures 2(a) and 2(b) present $\Delta\varepsilon^{hkl}$ as a function of σ_A for NC-Ni and NC-Co, respectively. In discussing $\Delta\varepsilon^{hkl}$, we focus on the $\Delta\varepsilon^{hkl}$ in the longitudinal direction (i.e., parallel to the loading direction). The tensile strain rate for NC-Ni is $\sim 4 \times 10^{-6}$ s^{-1}, and for NC-Co it is $\sim 6 \times 10^{-5}$ s^{-1}.

The elastic moduli of Ni for reflections 200, 220, 111, and 311 are 136 GPa, 232 GPa, 304 GPa, and 174 GPa, respectively. Under tensile stresses immediately following the onset of plastic deformation, $\Delta\varepsilon^{200}$ in coarse-grained (CG) Ni shows a tensile shift while $\Delta\varepsilon^{220}$ shows a compressive shift [4,8]. Surprisingly, this behavior is not reproduced in NC-Ni, where both $\Delta\varepsilon^{200}$ and $\Delta\varepsilon^{220}$ exhibit a compressive shift, suggestive of microscopic yielding in both orientations. Moreover, the behavior of NC-Ni is different from that previously reported for an NC-Ni-Fe alloy ($D \sim 9$ nm), in which both reflections show tensile shifts following yielding (presumably due to the "soft" GB phases) [4]. The plastic behavior in NC-Ni suggests that (1) dislocation mechanisms are activated, as indicated by 200 and 220 compressive shifts, (2) without considering the GBs, the deformation between different grain families in NC-Ni tends to yield together under the high stresses, and (3) the 0.2% yield stress ($\sigma_{0.2\%}$) may not be a good indicator of the macroscopic yielding in NC-Ni, as most grain families have not shown appreciable $\Delta\varepsilon^{hkl}$ at 0.2% strain [4,9]. Another important feature we observed in NC-Ni is that the 200 reflection shows more compressive shift than the 220 reflection at large strains, possibly due to a smaller volume fraction of {111} in-plane grains. Similar $\Delta\varepsilon^{hkl}$ behavior was observed in NC-Ni samples deformed at a strain rate of $\sim 3 \times 10^{-4}$ s^{-1}.

In contrast to the behavior seen in NC-Ni, $\Delta\varepsilon^{hkl}$ vs σ_A for NC-Co [Fig. 2(b)] displays very different features. With the exception of the 101 reflection, all other reflections we examined exhibit tensile shifts. The preferential yielding of the grains next to the 101 orientation is evident, as they exhibit a compressive shift and a decrease in their sharing of the macroscopic elastic strain. We notice that at $\sigma_{0.2\%}$, most reflections in NC-Co start to deviate from linear elasticity, suggesting that the 0.2% yielding criterion may be applicable for NC-Co. This distinct difference in macroscopic yielding behavior between NC-Ni and NC-Co suggests that GBs play critical roles in the microplasticity and macroplasticity of NC metals, as they share load repartition. In CG hcp Co, a dislocation slip is found to take place along the $\langle 110 \rangle$ close-packed directions on basal or prismatic planes, while twinning normally occurs on the $\langle 101 \rangle$ directions of the prismatic {102} planes. The dislocation slip and twinning lead to respective faulted stacking sequences, from $\ldots ABABABAB \ldots$ to $\ldots AB\mathbf{ABCA}CA \ldots$ (deformation faults) and $\ldots AB\mathbf{ABC}BCB \ldots$ (twin faults) (the local fcc stacking sequence is highlighted with bold letters). The $\Delta\varepsilon^{hkl}$ behavior of NC-Co (i.e., 101 compressive shift) suggests a tensile $\langle 101 \rangle \{102\}$ twinning mechanism that often occurs in hcp crystals with $c/a < \sqrt{3}$ (for Co $c/a = 1.623$).

For the case of twinning-related plastic behavior, the peak intensities from SXRD data are informative [10]. For

this reason, the evolution of the in-plane texture in both NC samples is quantified using two-dimensional polar plots. Here we define the texture index factor as $\Delta I^{hkl} = (I^{hkl} - I_0^{hkl})/I_0^{hkl}$, where I_0 and I refer to the peak intensity before and during tensile loading, respectively. Since we are comparing two NC metals with different slip/twinning systems, individual plane texture indices are preferred instead of average ones [7]. The ΔI^{hkl} for planes (101) and (002) of NC-Co, which exhibit the largest intensity changes, are shown in Figs. 3(a) and 3(b). The angle in the plots is the in-plane angle between the diffracting planes and the loading axis, where the azimuthal angle $\varphi = 0°$ is for planes parallel to the loading axis, and $\varphi = 90°$ is for planes perpendicular to the loading axis. The color bar reflects the changes of σ_A (i.e., red → green → blue). With increasing σ_A, the texture development in NC-Co is characterized by the strong buildup of (101) planes normal to the loading axis, a moderate decrease of (002) planes normal to the loading axis [suggesting the rotation of (002) planes away from the loading axis normal], and the reduction of the peak intensity of (110) planes along the transverse direction. We further observed that the increased (101) peak intensity remains after the sample fractures, suggestive of permanent residual defects. This behavior is in sharp contrast with that of NC-Ni [Fig. 3(c)] for which (200) shows the largest change in intensity, but is minimal compared to texture change in NC-Co. The lack of texture evolution in NC-Ni is in accordance with the previous work [7,11]. The development of strong {101} texture in NC-Co suggests that mechanical twinning has become an important factor contributing to the plastic deformation. In addition to the direct twinning shear strain contribution (a value of 0.119), twinning helps rotate the basal plane, increases the critical resolve shear stress for the dislocation slip, and consequently promotes further strain hardening.

Although twinning is a commonly observed deformation mode in CG hcp materials, this behavior is little known in the NC regime where twinning-mediated plasticity is considered to break down at a much larger crystal size due to the widespread observation that the Hall-Petch (H-P) slope for twinning is substantially larger than that for the dislocation slip [12]. A recent study in hcp materials indicates that twinning becomes less favorable when the crystal or sample size reduces below 1 μm [13]. Studies in NC-Ni also reveal an inverse D-dependent twinning behavior [14]. These results accentuate the importance of deciphering the twinning physics in hcp NC metals. We performed extensive high-resolution TEM (HRTEM) studies of the tensile-deformed samples and observed that the as-synthesized NC-Co has D in the range of ~7–55 nm (with some growth twins), as shown in Fig. 4(a). After tensile deformation, however, a larger portion of nanograins contain stacking faults and twins, an example of which is shown in Fig. 4(b). These nanotwins are coplanar in nature, with the two ends of twin boundaries sitting on the GBs, suggesting that GBs may be a promoter for twinning. The statistical D-dependent twinning probability shown in Fig. 4(c) indicates that the tendency for twinning in NC-Co attenuates when D decreases below ~15 nm. This behavior is likely due to the excessively high twinning stresses required for such smaller D, suggesting that the plastic deformation in NC-Co is inhomogeneous and carried principally by larger grains (> 15 nm).

The drastically different DMs suggested by SXRD and HRTEM data shed light on the different tensile properties observed in Fig. 1(b). The measured σ_y and the ultimate tensile stress for NC-Ni are 839 MPa and 1266 MPa, respectively, and for NC-Co they are 914 MPa and 1664 MPa, respectively. Note that the σ_y of NC-Ni observed here falls below the predicted value from the H-P relationship derived from the hardness data [15], which is

$$\sigma_y = 267\ \text{MPa} + 6.23\ \text{GPa} \cdot \text{nm}^{1/2}\, D^{-1/2}. \quad (1)$$

This may suggest a sample-size effect, or it is an indication that $\sigma_{0.2\%}$ is not a good measure of the macroscopic yielding in NC-Ni [4]. Assuming a dislocation-hardening mechanism, the flow stress increase in NC-Ni to the peak stress is $\Delta\sigma = 427$ MPa, which can be expressed as a Taylor-type hardening formula

$$\Delta\sigma = \alpha M G b(\sqrt{\rho} - \sqrt{\rho_0}), \quad (2)$$

where α is a hardening factor in the range ~0.3–0.6 (we use $\alpha = 0.5$), M is the Taylor factor (~ 3.06), G is the shear modulus of Ni (76 GPa), b is the Burgers vector

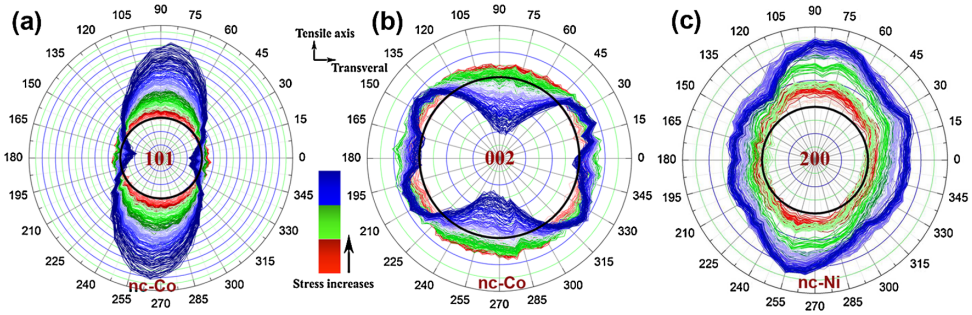

FIG. 3 (color online). Two-dimensional polar plots showing the change of (a) (101) and (b) (002) peak intensities for NC-Co, and (c) (200) for NC-Ni. The stress increment follows red (inside) → green (middle) → blue (outside) color. The solid black circles represent the initial intensity before loading. The blue circles represent a 5% increment in peak intensities.

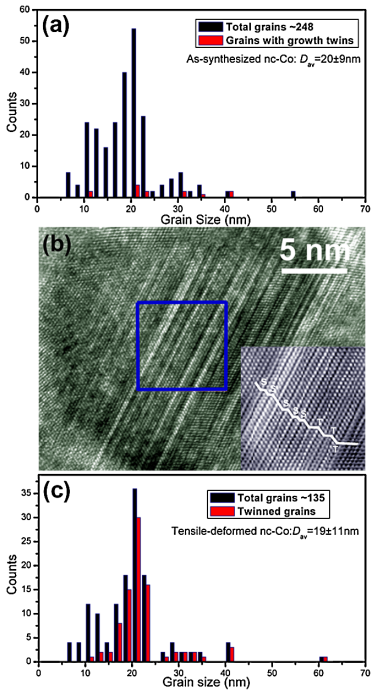

FIG. 4 (color online). (a) Statistical D distribution for as-synthesized NC-Co. (b) HRTEM image of deformation twins in NC-Co after tensile failure. The inset Fourier-filtered image is transformed from the square area. (c) Statistical D distribution of NC-Co and twinned grains after tensile deformation.

(0.249 nm), and ρ_0 and ρ are dislocation densities before and during loading, respectively. Using $\rho_0 = 4.7 \times 10^{15}$ m^{-2} [11], we obtain a ρ of 6.9×10^{15} m^{-2} at the peak load that is similar to the value of 6.5×10^{15} m^{-2} reported in Ref. [11] (assuming a lattice dislocation mechanism with a single b). The coincidence suggests that the strain hardening observed in NC-Ni is likely rendered by dislocation mechanisms [16]. On the other hand, the flow stress increase in NC-Co can be interpreted based on "twinning" and "effective D" concepts; i.e., the introduction of deformation twins is equivalent to the reduction of D and thus leads to a continuous increase of the flow stress. Using the data in Refs. [3,6], we derive a H-P formula of

$$\sigma_y = 432 \text{ MPa} + 1.90 \text{ GPa} \cdot \text{nm}^{1/2} D^{-1/2} \qquad (3)$$

for Co. At the peak stress, we estimate an effective D of ~2.4 nm. This is a low bound as the estimation did not consider the geometric and dislocation-hardening contributions. The results suggest that a high density of planar defects has been "pumped" into nanograins in order to sustain such high flow stresses.

Our results have implications for understanding and thereafter achieving large $\varepsilon_{\text{unif}}$ in truly NC metals. Although individual dislocation trapping has been observed in nanograins under tensile stresses [2,16], the buildup of large-scale dislocation networks has not been possible in materials with $D < 30$ nm, suggesting that sustainable strain hardening is not supported in NC metals with dislocation-hardening mechanisms. This behavior is in contrast with earlier investigations of materials with a fraction or all of the grains beyond 100 nm, where the dislocation storage remains feasible and thus large $\varepsilon_{\text{unif}}$ could be obtained [17–20]. In truly NC metals, our work instead hints at a new pathway for improving their tensile ductility; i.e., planar defect-related DM is an important and more effective avenue to render strain hardening in nanograins. This suggests that NC metals with the propensity for deformation faults or twins under tensile stresses may be intrinsically more ductile (e.g., NC-Co with a low stacking fault energy $\gamma_s = 27 \pm 4$ mJ/m^2 [17]). For NC metals with high γ_s (e.g., γ_s − Ni = 304 mJ/m^2 [18]), the addition of secondary or tertiary elements to reduce γ_s and promote deformation faults could prove to be a rewarding strategy to enhance the useful tensile ductility. We stress that the tactics of purposely inducing deformation twins or faults by resorting to cryogenic temperatures might not fare well, as low temperatures also drastically hike σ_y of NC metals [6], leaving little room for strain hardening [20].

This work was performed under the auspices of the U.S. DOE (DE-AC52-07NA27344) by Lawrence Livermore National Laboratory. The work at Ames Laboratory was supported by the Office of Basic Energy Sciences, U.S. DOE (DE-AC02-07CH11358). The APS was supported by the U.S. DOE (DE-AC02-06CH11357).

*ymwang@llnl.gov
†rtott@ameslab.gov

[1] J. R. Weertman *et al.*, MRS Bull. **24**, 44 (1999).
[2] K. M. Youssef *et al.*, Appl. Phys. Lett. **87**, 091904 (2005).
[3] A. A. Karimpoor *et al.*, Scr. Mater. **49**, 651 (2003).
[4] H. Q. Li *et al.*, Phys. Rev. Lett. **101**, 015502 (2008).
[5] X. L. Wu *et al.*, Phys. Rev. Lett. **103**, 205504 (2009).
[6] Y. M. Wang and E. Ma, Appl. Phys. Lett. **85**, 2750 (2004).
[7] S. Cheng *et al.*, Phys. Rev. Lett. **103**, 035502 (2009).
[8] B. Clausen, T. Lorentzen, and T. Leffers, Acta Mater. **46**, 3087 (1998).
[9] Y. M. Wang, A. V. Hamza, and T. W. Barbee, Appl. Phys. Lett. **91**, 061924 (2007).
[10] D. W. Brown *et al.*, Mater. Sci. Eng. A **399**, 1 (2005).
[11] Z. Budrovic *et al.*, Science **304**, 273 (2004).
[12] M. A. Meyers, O. Vohringer, and V. A. Lubarda, Acta Mater. **49**, 4025 (2001).
[13] Q. Yu *et al.*, Nature (London) **463**, 335 (2010).
[14] X. L. Wu and Y. T. Zhu, Phys. Rev. Lett. **101**, 025503 (2008).
[15] C. A. Schuh, T. G. Nieh, and H. Iwasaki, Acta Mater. **51**, 431 (2003).
[16] Z. W. Shan *et al.*, Phys. Rev. Lett. **98**, 095502 (2007).
[17] A. Korner and H. P. Karnthaler, Philos. Mag. A **48**, 469 (1983).
[18] H. Van Swygenhoven, P. M. Derlet, and A. G. Froseth, Nature Mater. **3**, 399 (2004).
[19] S. Cheng *et al.*, Acta Mater. **53**, 1521 (2005).
[20] See supplementary material at http://link.aps.org/supplemental/10.1103/PhysRevLett.105.215502 for additional information on grain size extraction, peak fitting, texture, and twinning.